PERGAMON

Journal of Quantitative Spectroscopy & Radiative Transfer 71 (2001) 157–168

Journal of Quantitative Spectroscopy & Radiative Transfer

www.elsevier.com/locate/jqsrt

Neon photoionization experiments driven by *Z*-pinch radiation

J.E. Bailey[a,*], D. Cohen[b,e], G.A. Chandler[a], M.E. Cuneo[a], M.E. Foord[d], R.F. Heeter[d], D. Jobe[c], P. Lake[c], D.A. Liedahl[d], J.J. MacFarlane[e], T.J. Nash[a], D. Nielson[a], R. Smelser[c], W.A. Stygar[a]

[a] *Sandia National Laboratories, P.O. Box 5800, Albuquerque, NM 87185-1196, USA*
[b] *Swarthmore College, Swarthmore, PA 19081, USA*
[c] *K-Tech Corporation, Albuquerque, NM 87185, USA*
[d] *Lawrence Livermore National Laboratory, Livermore, CA 94550, USA*
[e] *Prism Computational Science, Madison, WI 53703, USA*

Abstract

Present-day Z-pinch experiments generate $\sim 2 \times 10^{21}$ erg/s peak power, ~ 6 ns full-width at half-maximum X-ray bursts that provide new possibilities to study radiation-heated matter. This source is being used to investigate the production of plasmas in which photoionization dominates collisional ionization. Spectroscopic measurements of such plasmas can serve to benchmark atomic physics models of the photoionized plasmas. Beyond intrinsic interest in the atomic physics, these models will be applied to the interpretation of data from the new generation of satellite X-ray spectrographs that will promote the understanding of accretion-powered objects such as X-ray binaries and active galactic nuclei. Moreover, this information is needed for X-ray laser research. Our experiments use a 1-cm-scale neon gas cell to expose 10^{18} atoms/cm^3 to an X-ray flux of $\sim 5 \times 10^{18}$ erg/cm^2/s. Thin mylar (1.5 μm) windows confine the gas and allow the radiation to flow into the cell. The ionization is monitored with absorption spectra recorded with crystal spectrometers, using the pinch as a backlight source. In initial experiments we acquired an absorption spectrum from Li- and He-like Ne, confirming the ability to produce a highly ionized neon plasma. © 2001 Elsevier Science Ltd. All rights reserved.

Keywords: X-ray spectra; Photoionization; *Z*-pinch

1. Introduction

Many excellent spectroscopy experiments have been conducted in recent years to study atomic kinetics in plasmas where the ionization distribution and excited state populations are controlled

* Corresponding author. Tel.: +1-505-8457203.
E-mail address: jebaile@sandia.gov (J.E. Bailey).

0022-4073/01/$ - see front matter © 2001 Elsevier Science Ltd. All rights reserved.
PII: S0022-4073(01)00065-6

by electron collisions. In contrast, very few experiments have studied photoionized plasmas. Photoionized plasmas exist in a large class of astrophysical objects including X-ray binaries and active galactic nuclei. Spectra from photoionized plasmas represent a key for establishing the physics governing these objects [1] and are also important in X-ray laser research [2,3]. However, the interpretation of photoionized plasma spectra must presently rely on atomic kinetics models that have not been tested against laboratory experiments. In this paper we describe an experiment aimed at determining the feasibility of benchmarking atomic kinetics models with photoionized Ne plasmas produced by intense Z-pinch X-ray radiation.

There have been only a few photoionized plasma laboratory experiments reported previously. Time-resolved K-shell emission spectra from Ne photoionized by a sodium Z-pinch plasma were used to evaluate a photo-excitation approach to X-ray laser production [4], where the emphasis was on examination of population inversions, rather than on the acquisition of data suitable for testing atomic kinetics calculations. Moreover, experiments using laser-produced hohlraums to photoionize carbon plasma have also been reported [5]. The present work is a companion effort to studies of the production of photionized iron plasmas [6].

The paucity of data from laboratory photoionized plasmas is due mainly to the need for a high-intensity radiation source, as the incident radiation field must be intense enough so that photoionization dominates over collisional processes. For testing astrophysics models the ionization conditions must be comparable to astrophysical regimes which translates into radiation fields high enough to yield dominant photoionization and into densities low enough so that 3-body recombination is small compared to dielectronic and radiative recombination. The incident radiation field and the plasma density and temperature that are produced must all be measured, preferably without resorting to either hydrodynamics models or to spectroscopic analysis that relies on the atomic model that is being tested. Further, the plasma must be uniform enough so that the gradients resulting from integration along the spectroscopic line of sight do not affect the result. Finally, the duration of the experiment should be long enough that recombination equilibrates with the photoprocesses.

Meeting all of the requirements outlined above is clearly a challenging assignment. The main goal of the present work is to evaluate whether a photoionized plasma can be produced and diagnosed using the gas cell method on ride-along experiments at the Sandia National Laboratories Z facility [7–9]. The Z facility is presently the most energetic X-ray source in the world, producing Z-pinch plasmas that emit up to 1.2 MJ of X-rays. Here, a "ride-along" experiment means that we use the radiation produced by an experiment with another primary goal, such as Z-pinch physics investigations. Using ride-alongs has the advantage that initial scoping studies can be performed without the cost associated with dedicated experiments. The disadvantage is that the ride-along must be designed to avoid compromising the primary experiment and that the radiation available is not necessarily optimized. Despite these drawbacks, we have succeeded in fielding neon gas cells in close enough proximity to the Z radiation source to produce photoionized Ne plasma. Using the pinch as a backlighter, we obtained absorption spectra clearly demonstrating the presence of Li- and He-like Ne in the plasma. This confirms the potential of the gas cell approach, but further work is needed in order to satisfy the many requirements for benchmarking atomic kinetics models.

2. Experiment

The experiments described in this paper use a Z-pinch radiation source created by delivering the 20 MA current from the Z accelerator to a cylindrical annular array of tungsten wires. The current flowing through the wires converts them into plasma and then compresses the plasma onto the cylinder axis. Upon stagnation, the plasma emits copious X-rays. The X-ray source can be roughly characterized as a 2-cm tall, 0.2-cm diameter blackbody with a temperature that typically peaks at approximately 200 eV. The return path for the current that flows through the Z-pinch plasma is a gold-coated stainless-steel 5-cm-diameter cylinder that surrounds the pinch. Slots cut into this cylinder permit diagnostic access to the pinch plasma and provide capability to expose samples to the pinch radiation. We exploit the radiation produced in these experiments by locating a gas cell between the Z-pinch radiation source and a time-integrating space-resolved convex crystal X-ray spectrometer. The pinch radiation source serves to heat, photoionize and backlight the plasma. A schematic diagram of the experimental setup is shown in Fig. 1.

To characterize the radiation intensity we use the ionization parameter defined in the astrophysics literature [10,1] as $\xi = 4\pi I/N$, where I is the irradiance at the sample expressed in erg/cm^2/s. In common usage N is the ion density, typically approximately the same as the electron density for astrophysical plasmas; however, here we use the electron density, since this equation is intended to reflect the balance between photoionization and recombination. The regime of interest [1] is $\xi \sim 1$–1000 erg cm/s. Lower values of ξ are of interest for relatively low atomic number (Z) species while higher values are more interesting for higher-Z elements. The ionization parameter in the experiments described here is approximately 7 erg cm/s.

Laboratory photoionized plasma experiments require the production of relatively low-density plasma, since the radiation intensity needed to reach a desired value of the ionization parameter is lower. Further, for astrophysics model comparisons, a density as low as possible is desirable since the density encountered in astrophysics applications is typically 10^8–10^{13}/cm^3. There are

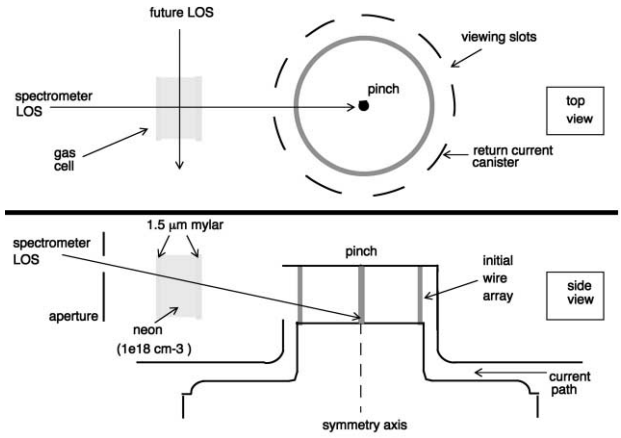

Fig. 1. Schematic diagram of the experiment.

two general approaches to generating the low-density plasma. The approach used by Heeter et al. [6] to study iron plasmas is to preheat a tamped thin foil with a low-intensity X-ray source so that the foil expands to the desired density prior to the application of the main photoionizing radiation field. This is by far the most straightforward way to study metallic elements, or any other element that occurs naturally as a solid. The main disadvantage is the dynamic nature of exploding foil experiments. The approach described here is to use a gas cell that is filled to the desired atom density. This has the advantage that the atomic density is known and is easily adjusted to be quite low. It allows study of gaseous materials, including mixtures. The main disadvantage is that a thin window (typically a CH foil) must contain the gas and the hydrodynamic expansion of this window may affect the gas cell plasma. Our view is that the expanding foil and gas cell approaches are complementary and both warrant further investigation.

The design of photoionized gas experiments involves consideration of conflicting requirements. First, we want to maximize the incident radiation in order to achieve interesting values of the ionization parameter. This motivates us to locate the gas cell as close as possible to the radiation source. However, we also want uniform conditions within the cell. In the present experiment we are using the pinch plasma as the backlight source for absorption spectroscopy and are thus integrating along the radial direction through the cell. This implies that we want to place the cell as far as possible from the source, so that geometric dilution does not cause appreciable variation in the radiation intensity throughout the cell. Note that the use of an independent backlighter plasma to view along a chord perpendicular to the radius would alleviate this problem, since then the radial extent of the plasma that is actually used is small (e.g., see the "future LOS" in Fig. 1). The second consideration involves the density. Lower densities provide a higher ionization parameter and are closer to the astrophysics regime. However, higher electron densities decrease the time scale for recombination to equilibrate with photoionization and thus may enable comparison with steady-state kinetics models. The third consideration relates to the size of the gas cell. A large cell promotes hydrodynamic isolation, so that the plasma information obtained reflects the photoionized plasma in the cell interior, not the region influenced by the cell windows or walls. Large cells also enable the acquisition of absorption spectra at lower densities. However, if the cell is too large, then uniformity may be degraded. These three considerations require compromises given the existing radiation source. It is clear that the more intense the radiation source is the more flexibility exists in the experiment design and the closer we can come to achieving ideal conditions.

In this experiment we used a $1 \times 2 \times 2.34$-cm gas cell, with the 1-cm dimension oriented along the radial line of sight (LOS) to the pinch and the 2-cm dimension oriented perpendicular to the plane formed by the radial line of sight and the pinch axis. The front, rear, and one side consisted of 1.5 μm mylar windows held by a stainless-steel frame with an o-ring seal. The window material was chosen to ensure robust cell operation, balanced by the desire to allow radiation to flow with minimal attenuation into the cell. We point out that thinner windows are probably feasible, but for these initial ride-along experiments, freedom from gas leaks into the region around the pinch was of paramount importance. The front window surface was located 57 mm from the pinch axis. This distance was a compromise between the desire for uniform conditions and high radiation intensity. The cell was filled with 30 Torr of Ne, equivalent to 1.06×10^{18} atoms/cm^3. This density is at the upper limit for photoionization to dominate the

ionization process. Lower densities are feasible, but the time scale for equilibrium between recombination and photoionization may then exceed the duration of the radiation pulse. The gas cell size was dictated by the need for hydrodynamic isolation and to obtain measurable absorption lines. Preliminary calculations with a one-dimensional Lagrangian radiation hydrodynamics computer code [11] indicated that the gas cell is big enough to isolate the central $\sim$8 mm of the cell from boundary effects, such as shock waves launched at the windows. These results will be published elsewhere.

Characterization of the pinch radiation field is an essential aspect of any experiment seeking to improve understanding of radiation matter interaction. The radiation on Z is measured with a diagnostic suite that has been described in detail elsewhere [12–16]. The pinch radiation can be divided into two phases: the run-in and final stagnation. The run-in corresponds to the emission as the annular wire array is compressed from its 2-cm initial radius onto the pinch axis. It lasts for about 100 ns and the brightness temperature rises from approximately 20 eV at the beginning to 50 eV just prior to stagnation. The final stagnation typically creates a 6 ns full-width at half-maximum (FWHM) X-ray burst with a power reaching as high as 280 TW and a spectrum that corresponds roughly to a 200 eV blackbody. The total X-ray energies, peak powers, and burst FWHM in the experiment reported here were 1.45 MJ, 135 TW, and 7.5 ns, respectively. In addition to this quasi-blackbody radiation, the pinch stagnation also produces tungsten M-shell emission in the 2–3 keV photon energy regime. Typically, this M-shell emission accounts for roughly a few percent of the total radiation emission. Despite this low percentage, the emission of tens of kJ of multi-keV radiation could be significant for photoionization studies of elements with high ionization potentials.

The radiation field experienced by plasma within the gas cell is calculated from the measured pinch emission using a view factor code [17]. There are two main reasons why view factor calculations are essential. The first is geometrical dilution. This refers to the calculation of radiation intensity as a function of position, taking the three dimensional geometry of the pinch radiation source into account. In general this is a time-dependent problem, since the pinch source position changes during the run-in. The initial wire radius is 2 cm, a significant fraction of the distance from the final pinch location to the sample. According to simulations the wire plasma moves little during the first 50 ns of the experiment. These factors tend to increase the importance of run-in radiation above what one might conclude given the low temperature during the run-in compared to the stagnation. This time dependence is less important during the stagnation, since the pinch size change is small compared to the distance between the pinch and the sample. Note that the geometrical dilution is different for the front of the gas cell compared to the back and the view factor calculations permit us to evaluate the anticipated uniformity of the radiation conditions.

The second reason for using the view factor calculations is that the cell is exposed to re-emission from the electrode walls, ceiling, and floor surrounding the pinch. The wall re-emission typically accounts for 25–50% of the radiation experienced by a sample. In addition, this alters the composite spectrum incident on the sample, since the pinch radiation contributes the equivalent of a diluted 200 eV blackbody, while the spectrum from the wall re-emission varies over the 75–200 eV temperature range, depending on how close the wall segment is to the pinch. Typical transmission grating spectrometer [16] measurements of the output spectrum from the pinch and the side wall of the return current canister are shown in Fig. 2. We emphasize that

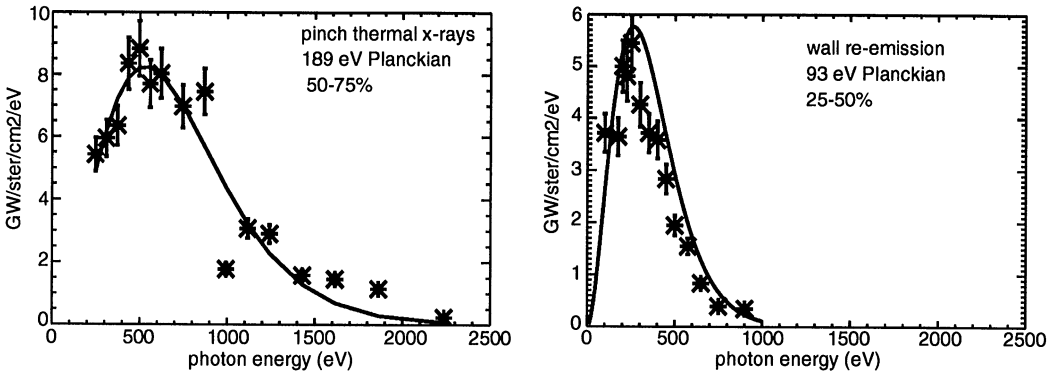

Fig. 2. Transmission grating spectra measured at peak power in a similar Z experiment. Two separate instruments are used to measure the pinch and wall re-emission radiation.

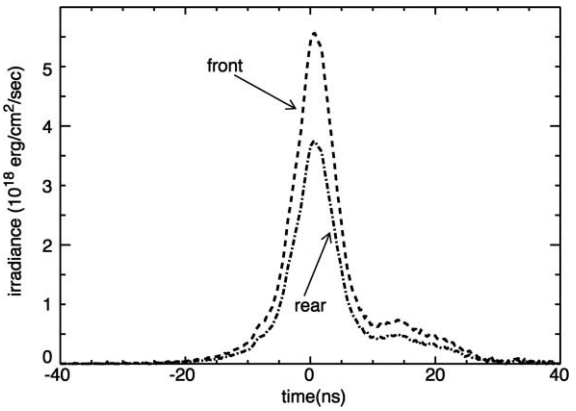

Fig. 3. Incident radiation at the front and rear gas cell windows computed with the view factor code from the measured pinch output power.

the wall re-emission varies according to the closeness of the wall element under consideration to the pinch. The complexity of converting the measured pinch emission into the irradiance experienced by the gas cell makes it imperative to verify the accuracy of the sample irradiance. Additional absorption spectroscopy experiments using benchmarked analysis of a collisional aluminum plasma exposed to the pinch radiation confirm the validity [18] of the method described here. Evaluation of the irradiance uncertainty in the present gas cell experiments is in progress.

The irradiance incident onto the gas cell calculated with the view factor code from the measured pinch power is shown in Fig. 3. For this experiment a single view factor calculation at the time corresponding to peak power was performed, using albedos computed in self-consistent radiation hydrodynamics/view factor calculations [17]. The total irradiance at the front gas cell window was found equivalent to a 48.3 eV blackbody, although the spectrum was a convolution of the pinch and wall re-emission spectra, as noted above. The irradiance at the rear gas cell

boundary was calculated to be a factor of 1.5 lower, or equivalent to a 43.7 eV blackbody. The time history of the irradiance at the gas cell was then estimated by assuming that the dilution of the source radiation and the albedos were constant with time. These approximations were judged sufficient for the initial experiments reported here, but the more complete treatment described in Ref. [17] is necessary for future detailed model comparisons.

The principal gas cell diagnostics in these experiments were two space-resolved time-integrated convex crystal spectrometers. The LOS was configured so that the pinch acted as a backlighter, in addition to heating the sample. The LOS viewed the pinch through the gas cell at a 78° angle to the pinch axis. A 3.5-mm-tall aperture limited the field of view of the spectrometer to a restricted region inside the gas cell. This reduced the signal available for recording by the spectrometer, but is necessary to ensure that we sample uniform conditions within the gas. The view factor calculations described above confirm the expectation for uniformity in the dimensions perpendicular to the line of sight, within the spectrometer field of view. Spatial resolution was provided by two slits for each spectrometer. One spectrometer was oriented to obtain resolution in the axial direction along the pinch and the other was oriented to obtain spatial resolution in the radial direction, perpendicular to the pinch axis. The source-to-slit and source-to-detector distances were 303.9 and 453.6 cm, respectively. The magnification was thus 0.5. The axial instrument used 0.2 and 0.25 mm slits to achieve spatial resolution of 0.6–0.75 mm and the radial instrument used 0.36 and 0.56 mm slits to achieve 1.1–1.68-mm resolution. Both instruments used the (0 0 1) plane of KAP bent to a 2.54-cm-radius. A 12.5-μm-thick Be filter placed in front of the crystal prevented visible light from reaching the detector. The detector was a strip of Kodak DEF X-ray film, curved to lie 85 mm from the intersection of the LOS with the crystal. Lead collimating baffles and shields were employed to minimize the fogging due to hard X-rays created by the accelerator.

3. Results

A radially resolved spectrum is shown in Fig. 4. Although the detector is time-integrated, the use of the pinch as a source for absorption spectroscopy implies that the spectrum represents plasma conditions during the ~7-ns period associated with the pinch stagnation emission. The spectrum consists of a quasi-continuum from approximately 6.5–20 Å together with tungsten M-shell lines and unresolved transition arrays in the 4–7 Å range. The tungsten M-shell features are from Ni-like and adjacent charge state ions. Analysis of these features would be valuable but is beyond the scope of this paper. The spectrum is imaged such that we observe the radial extant of the pinch emission as a function of wavelength, integrated over the spectrometer field of view along the pinch axis. The quasi-continuum originates from the ~2-mm-diameter of the *Z*-pinch core, while the tungsten M-shell emission extends to larger radii. In principle, the radial imaging enables us to determine whether any self-emission from the gas cell contributes to the spectrum, since the pinch emission is restricted to relatively small radii but the gas cell self-emission should arise from the entire gas cell. No self-emission was observed, mainly because this spectrometer is designed to measure the intense radiation from the pinch without saturating and it consequently has insufficient sensitivity to record the gas cell emission.

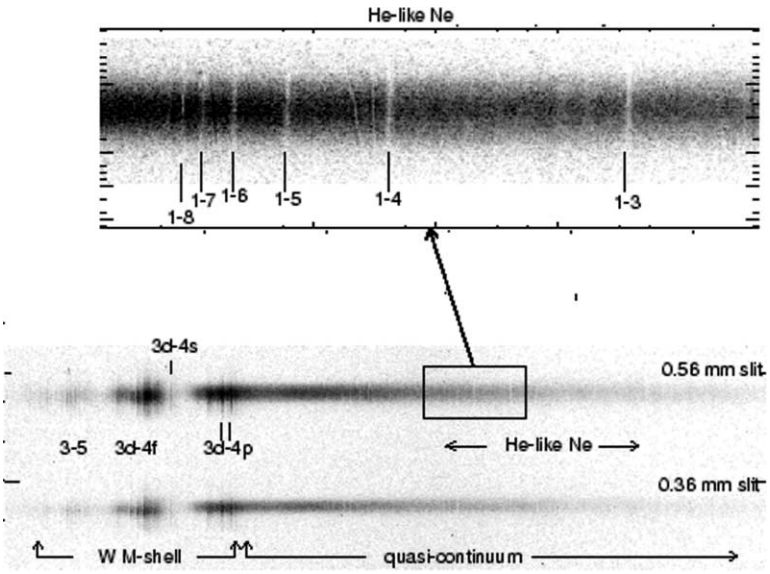

Fig. 4. Radially resolved absorption spectrum from Z experiment #543. Two slits are used to produce the spatially resolved spectra. The wavelength range covers approximately 4–15 Å . The inset is an enlarged view of the 10–11.5 Å region.

Absorption features from the neon plasma are clearly visible in the spectra. A lineout averaging over the 0.56-mm-slit spectrum is shown in Fig. 5. The data processing began by subtracting the chemical film fog to obtain net film density above fog. We then apply a wavelength scale using the instrument geometry, with the Ne IX He β line serving as the reference. We unfold the film response using the film calibration measured by Henke et al. [19]. We correct for the light tight filter transmission, the instrument geometry, and the crystal reflectivity using Refs. [20,21], respectively. A second lineout was taken outside the region of the pinch emission as an approximate measure of the background due to bremsstrahlung, scattered X-rays, and crystal fluorescence. This background was smoothed and then subtracted from the lineout containing the pinch emission and gas cell absorption. The film correction applied to the signal lineout was applied to the background lineout, even though the crystal does not disperse the photons inducing the background so that the energy scale is incorrect. The errors introduced by this procedure were discussed in Ref. [22] and for the present case the error is negligible for wavelengths below $\sim$12 Å as the pinch radiation signal is much larger than the background. However, the increasing attenuation by the light tight filter at wavelengths beyond 12 Å reduces the signal from the pinch to levels that are only $\sim$4 times larger than the background. This may lead to errors in the Ne He α signal intensity.

Once the spectrum is corrected for film response, instrument sensitivity, and background we convert the absorption spectrum into a transmission measurement for the gas cell plasma using the following procedure. An independent measurement of the un-attenuated pinch spectrum was not available so we approximate by removing the absorption peaks. We then apply a low-pass filter to the remaining data to obtain a smoothly varying representation for the un-attenuated

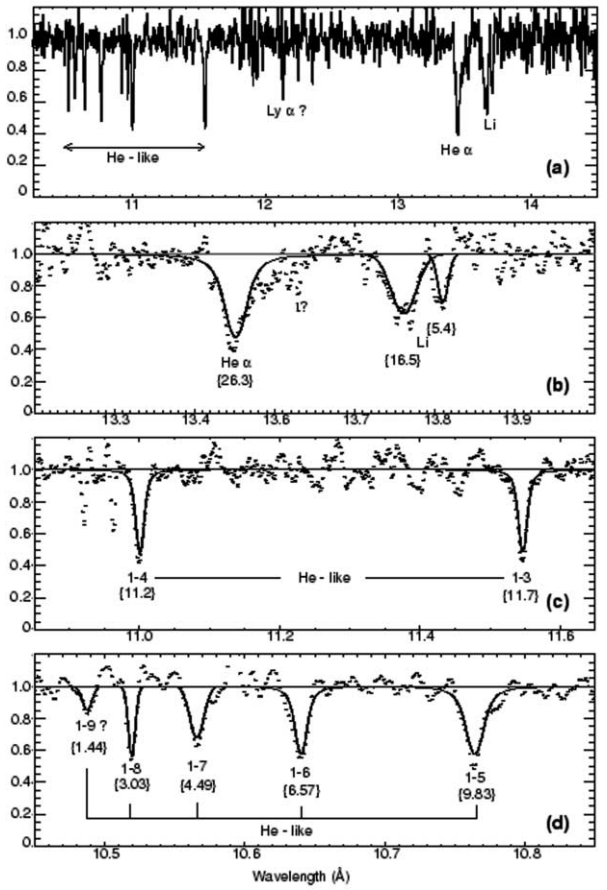

Fig. 5. Transmission determined from the absorption spectrum shown in Fig. 4. The top plot shows data from the 10–14 Å region where the neon absorption features appear. The lower three plots show enlarged views of the data (displayed as dots) with fits to the peaks (solid lines) superimposed. The equivalent widths in mÅ determined by fitting with ROBFIT are shown in brackets below each peak.

spectrum. The original data is then divided by this smooth spectrum to obtain the approximate transmission through the gas cell plasma. The transmission determined by this method is displayed in Fig. 5a. The He- and Li-like Ne lines are clearly visible in this spectrum. There is also a feature that appears at the hydrogen-like neon Lyα wavelength. However, we are unsure that this feature is a real absorption line, or if it is simply an artifact due, for example, to a film or crystal defect.

The relative intensities of the neon absorption lines were determined using the ROBFIT line fitting code [23]. The fits to the absorption lines are superimposed on the data in Fig. 5b–d. The intensities measured with the ROBFIT code are expressed as equivalent widths (as defined below) in Fig. 5. The code was operated in a mode that uses the fluctuations within the data itself to determine the uncertainties, assuming that the data obey Poisson statistics. The method we used to determine the transmission, along with the possibility of inaccurate background

subtraction, may render this assumption invalid and we consequently regard these intensities as preliminary.

4. Discussion

The main result of the work presented here is that photoionized gas ride-along experiments using the Z radiation source are feasible. The statement that this is a photoionized plasma relies on previously published analysis [2,3] along with the conditions in this experiment. The exact relative importance of photoionization and collisions needs to be evaluated in future analysis and measurements. There are two major questions regarding these results. First, what information on the underlying physical processes can be extracted from the absorption spectra we have already acquired? Second, what improved measurements are needed to benchmark atomic kinetics models?

We believe the present absorption spectra are suitable for determining the charge state distribution and possibly the plasma temperature. We observe absorption lines from He- and Li-like Ne transitions. The He-like $1s^2$–$1snp$ series up to $n = 8$ is observed, while only $n = 1$–2 transitions in the Li-like ions are seen. No lines from Be-like or lower charge state ions are observed. Further, there is a weak signature that may be the Ne X Lyα transition, but the intensity is too low to be certain it is not an artifact. These facts immediately place qualitative bounds on the charge state distribution: the plasma consists of mostly Ne IX and Ne VIII.

A quantitative determination of the charge state distribution must take line saturation into account. The areal density of the He-like ground state is approximately $n_l l \sim 9 \times 10^{17}\ \mathrm{cm}^{-2}$, where for the purposes of this estimate we have assumed that 80% of the initial gas atoms are in the He-like ground state. For the temperature range of interest, 10–100 eV, the Doppler widths are $\sim$1 mÅ so that the line center optical depths for the Ne IX $1s^2$–$1snp$ transitions range from 10^1 to 10^3. Furthermore, our present spectral resolution is approximately $\lambda/\delta\lambda \sim 1000$, a factor of 10 broader than the anticipated line widths. Therefore, it is clear that the absorption lines should be strongly saturated.

A quantitative analysis can be performed using a radiation transport code to compute synthetic spectra for comparison with the data, taking into account the line oscillator strengths and widths, the instrument response, and the known total atomic areal density. As an alternative, our situation is reminiscent of many astrophysical spectra, where the instrument resolution is incapable of resolving the lines. This similarity suggests that it may be useful to employ the well-known curve of growth method [24]. Briefly, this method uses the equivalent widths W_l of the lines to extract information about the plasma from the spectra. W_l is defined as the width of a rectangle with area equal to the area under the absorption line. A plot of log W_l vs. log $(n_l f l)$ is known as the curve of growth, where f is the transition oscillator strength and $n_l l$ is the lower level areal density. We can generate such a plot by computing W_l for the Ne IX multiplet since the lines originate from the same lower level, but the oscillator strengths vary by a factor of 84 between the $1s^2$–$1s2p$ and $1s^2$–$1s8p$ transitions. This should enable a determination of the absolute He-like Ne ground state density.

In addition, the curve of growth provides a measurement of the Voigt parameter $a = 1.414(\delta\lambda_\mathrm{L}/\delta\lambda_\mathrm{D})$, where $\delta\lambda_\mathrm{L}$ is the Lorentzian FWHM and $\delta\lambda_\mathrm{D}$ is the Doppler FWHM.

This is because the line profile plays an important role in determining the way that the absorption line saturates. For a Gaussian line, the absorption near line center is a relatively large fraction of the total absorption. For a Lorentzian, the wings play a bigger role. Thus, a Gaussian line begins to saturate at a lower value of the $n_l f l$ product than a Lorentzian line, since the peak line strength is larger. This produces a dependence of the curve of growth on the Voigt parameter a. Once a is determined, we can solve for $\delta\lambda_D$ and thus T_i, assuming the Lorentzian portion of the line width is known. The Lorentzian part of the line broadening in our situation is mainly due to natural broadening, although the possibility of Stark broadening contributing to the higher n transitions must be carefully evaluated. The electron temperature can be determined under the assumption that $T_e \sim T_i$.

The accuracy of any quantitative analysis depends on the experimental measurements of the line intensities. The main concerns are background subtraction and the difficulty in measuring the intensity in the line wings. An additional source of possible uncertainty in the measurements results from Bragg diffraction from the (0 1 3) KAP crystal plane. This plane is not parallel to the (0 0 1) cleavage plane and it is known to contribute to convex crystal spectra [25]. The $2d$ spacing for this plane is 8.061 Å . The difference in the $2d$ spacing and the angle between the crystal planes imply that ~6-Å X-rays diffracted from the (0 1 3) plane can overlap with ~13-Å X-rays diffracted from the (0 0 1) plane. Quantitative conclusions based on these data, particularly at the longer wavelengths where this problem tends to be more important, should be regarded with caution until this issue can be resolved.

The observed spectra confirm the ability to produce Li- and He-like Ne charge states. Most likely these charge states are produced primarily by photoionization. The measurements of the incident radiation field that induces this ionization are probably adequate [18]. However, the characterization of the neon plasma needs extensive work before data will be available that can stringently constrain atomic kinetics models. Temperature measurements using the curve of growth method described here will be useful, but additional results from emission spectroscopy measurements of the free-bound continuum or Thomson scattering would improve the accuracy. Time- and space-resolved interferometry measurements of the electron density would help to ascertain the uniformity of the gas cell plasma and to evaluate the possible importance of shock waves created at the gas cell windows. The present results provide a basis for designing these future improved experiments.

Acknowledgements

Sandia is a multiprogram laboratory operated by Sandia Corporation, a Lockheed Martin Company, for the United States Department of Energy under contract DE-AC04-94AL85000. The authors thank the Z accelerator team for excellent assistance in performing the experiments. Continuous support and encouragement was provided by R.J. Leeper and M.K. Matzen.

References

[1] Kallman TR, McCray R. Astrophys J Suppl Ser 1982;50:263.

[2] Apruzese JP et al., In: Tallents GJ, editor. Proceedings of the Second International Colloquium on X-ray Lasers, York, England, Bristol, Institute of Physics, 1991, p. 39.
[3] Nilsen J, Chandler E. Phys Rev A 1991;44:4591.
[4] Porter JL et al. Phys Rev Lett 1992;68:796.
[5] Morita Y et al. JQSRT 2001;71:519, this issue.
[6] Heeter RF et al. Rev Sci Instr 2001;72:1224.
[7] Matzen MK. Phys Plasmas 1997;4:1519.
[8] Spielman RB et al. Phys Plasmas 1998;5:2105.
[9] Matzen MK. Fusion Eng Design 1999;44:287.
[10] Tarter CB, Tucker W, Salpeter EE. Astrophys J 1969;156:943.
[11] MacFarlane JJ, Moses GA, Petersen RR. Report # UWFDM-984, University of Wisconsin, 1995.
[12] Nash TJ et al. Rev Sci Instr 2001;72:1167.
[13] Idzorek GC, Bartlett RJ. In: Siegmund OHW, Gummin Ma, editors. EUV, X-ray, and gamma-ray instrumentation for astronomy VIII, SPIE Proceedings Vol. 3114, 1997, p. 349.
[14] Chandler GA et al. Rev Sci Instr 1999;70:561.
[15] Spielman RB et al. Rev Sci Instr 1997;68:782.
[16] Ruggles LE, Porter JL, Bartlett R. Rev Sci Instr 1997;68:1063.
[17] MacFarlane JJ et al. Rev Sci Instr 2001;72:1228.
[18] MacFarlane JJ, Bailey JE, 2001, in preparation.
[19] Henke BL et al. J Opt Soc Am B 1986;3:1540.
[20] Henke BL, Yamada HT, Tanaka TJ. Rev Sci Instr 1983;54:1311.
[21] Henke BL, Private communication.
[22] Gorzen DF et al. Rev Sci Instr 1990;61:2768.
[23] Coldwell RL, Bamford GJ. The theory and operation of spectral analysis using ROBFIT. New York: American Institute of Physics, 1991.
[24] Aller LH, The atmospheres of the sun and stars, New York: Ronald Press, 1963, p. 369.
[25] Burkhalter PG, Brown DB, Gersten M. J Appl Phys 1981;52:4379.